The Journal of Pathology: Clinical Research
J Pathol Clin Res July 2018; **4:** 167–174
Published online 13 June 2018 in Wiley Online Library (wileyonlinelibrary.com). DOI: 10.1002/cjp2.104

ORIGINAL ARTICLE

Atypical tuberous sclerosis complex presenting as familial renal cell carcinoma with leiomyomatous stroma

Ismaël Bah[1], Somayyeh Fahiminiya[2,3], Louis R Bégin[4], Nancy Hamel[2], Maria D D'Agostino[5,6], Simon Tanguay[7] and William D Foulkes[2,5,8,9]*

[1] *Department of Pathology, McGill University Health Centre, Montreal, QC, Canada*
[2] *Cancer Research Program, Research Institute of the McGill University Health Centre, Montreal, QC, Canada*
[3] *Génome Québec Innovation Centre, McGill University, Montreal, QC, Canada*
[4] *Division of Anatomic Pathology, Hôpital du Sacré-Coeur de Montréal, Montreal, QC, Canada*
[5] *Department of Human Genetics, McGill University, Montreal, QC, Canada*
[6] *Department of Medical Genetics, McGill University Health Center, Montreal, QC, Canada*
[7] *Division of Urology, McGill University Health Center, Montreal, QC, Canada*
[8] *Department of Medical Genetics, Lady Davis Institute, Segal Cancer Centre, Jewish General Hospital, Montreal, QC, Canada*
[9] *Program in Cancer Genetics, Department of Oncology and Human Genetics, McGill University, Montreal, QC, Canada*

**Correspondence to: William D Foulkes, Department of Medical Genetics, Lady Davis Institute, Segal Cancer Centre, Jewish General Hospital, 3755 Cote St. Catherine Road, Montreal, QC, Canada H3T 1E2. E-mail: william.foulkes@mcgill.ca*

Abstract

We report an atypical tuberous sclerosis complex (TSC) phenotype presenting as familial multiple renal cell carcinomas (RCCs) with (angio)leiomyomatous stroma (RCCLS) (5/7 familial RCCs) on a background of multiple angiomyolipomas, hypopigmented skin macules, and absence of neurological anomalies. In the index case and three relatives, germline genetic testing identified a heterozygous *TSC2* missense pathogenic variant [c.2714 G>A, (p.Arg905Gln)], a rare TSC-associated alteration which has previously been associated with a milder TSC phenotype. Whole-exome sequencing of five RCCs from the index case and one RCC from his mother demonstrated either unique tumour-specific deleterious second hits in *TSC2* or significant allelic imbalance at the *TSC2* gene locus (5/6 RCCs). This study confirms the key tumourigenic role of tumour-specific *TSC2* second hits in TSC-associated RCCs and supports the notion that RCCLS may be strongly related to abnormalities of the mTOR pathway.

Keywords: tuberous sclerosis complex; renal cell carcinoma; TSC2; renal cell carcinoma with (angio)leiomyomatous stroma; renal angiomyoadenomatous tumour

Received 28 February 2018; Revised 4 April 2018; Accepted 9 April 2018

No conflicts of interest were declared.

Introduction

Tuberous sclerosis complex (TSC) is an autosomal dominant genetic disorder characterised by hyperplastic, dysplastic, and hamartomatous lesions in various tissues. Its frequency is estimated at 1 in 6000 live births, 65% of cases being sporadic [1]. Disease results most frequently from inactivating alterations of tumour suppressor genes *TSC1* and *TSC2*, respectively, encoding proteins harmartin and tuberin, which normally regulate protein synthesis and cell growth via the mTOR pathway. Genetic alterations resulting in constitutively active mTORC1 signalling drive cell hyperplasia and dysplasia in TSC patients, with the development of variably severe phenotypes. The skin, brain, kidney, heart, and eyes are the organs most frequently involved [2].

We report the case of a 52-year-old man originally referred to the medical genetics service because of a personal and familial history of renal cancer. Our index patient first came to medical attention for a history of right flank pain appearing at age 33 and lasting over a year, with a subsequent computed tomography (CT) scan disclosing multiple bilateral kidney lesions, among which there were six right cortical lesions including a dominant 2 cm upper pole nodule. The latter lesion was resected in 2000

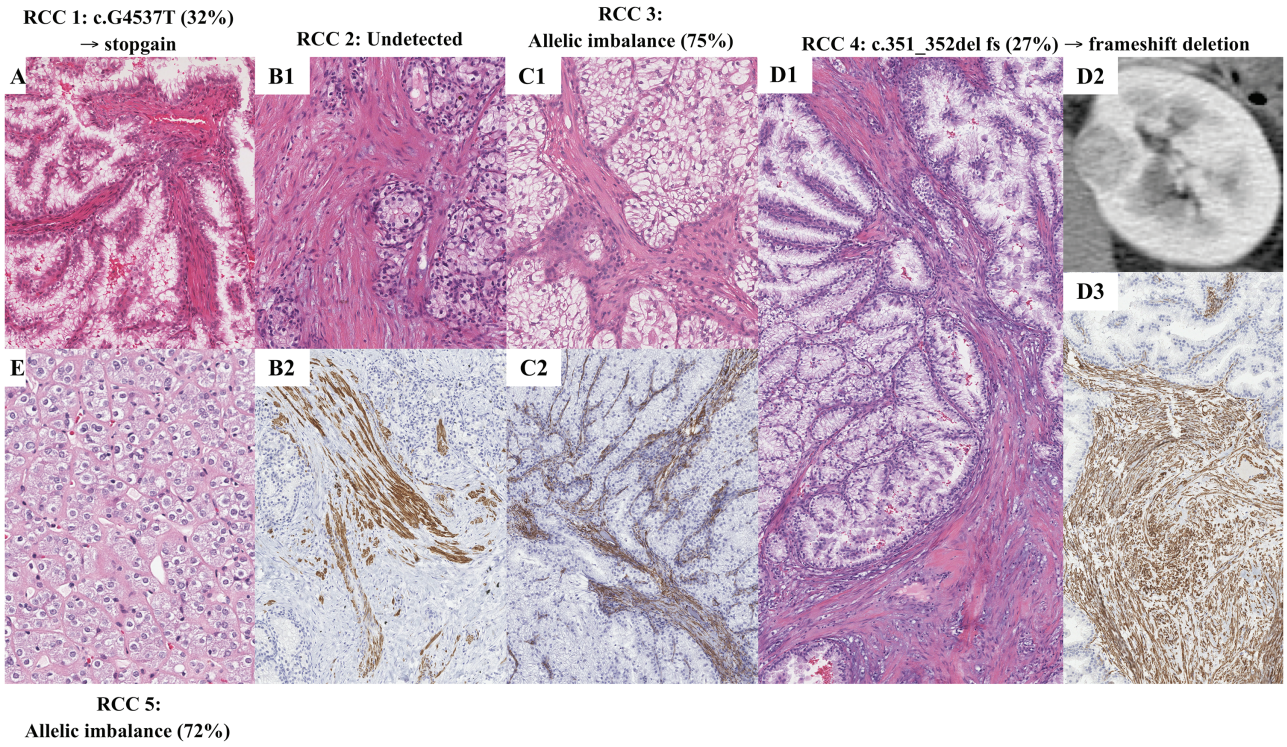

Figure 1. Multiple RCCs resected in the proband to date, alongside corresponding genetic alterations detected by WES. Four RCCLS all demonstrate a clear cell papillary growth pattern with focally aggregated stromal smooth muscle fibres (A, B1, C1, D1; H&E stains). Stromal smooth muscle cells are highlighted using leiomyomatous immunohistochemical markers such as desmin (B2), muscle-specific actin (C2), and smooth muscle actin (D3). All these RCCLS tumours displayed IHC positivity for CK7, CD10, CAIX, and vimentin (both epithelial and stromal positivity; data not shown). The largest among the left-sided RCCLS tumours reached 1.5 cm in size, displaying heterogeneous contrast uptake on computed tomography imaging (D2; 2008 CT Scan with contrast, nephrogenic phase). The right kidney lesion excised at age 42 corresponded to a chromophobe-like RCC composed of nests/tubules of cells with irregular nuclear membranes ('raisinoid' nuclei), perinuclear cytoplasmic clearing, granular eosinophilic cytoplasm, conspicuous cytoplasmic membranes, and thick eosinophilic septa separating cell groups (E).

and was diagnosed as a renal cell carcinoma with (angio)leiomyomatous stroma (RCCLS; Figure 1A). Follow-up CT scan in April 2008 at age 42 disclosed a growing 1.5 cm solid left kidney mass, along with ipsilateral concurrent smaller lesions, warranting a left partial nephrectomy which revealed four RCCLS tumours associated with one lymph node metastasis and background multifocal angioleiomyomas (mainly leiomyomatous; Figure 1B–D). A concurrent 1.5 cm right kidney solid nodule with an ipsilateral 1.5 cm cyst were also noted, while positron emission tomography and CT imaging revealed multiple bony lesions, stable up to this day, which are probably TSC-associated sclerotic bone lesions (SBL) (supplementary material, Figure S1) [3]. Seven infracentimetric ground glass pulmonary opacities were also noted at the time and remained stable in size, most likely corresponding to multifocal micronodular pneumocyte hyperplasia (supplementary material, Figure S2). In August 2008, a right partial nephrectomy led to a diagnosis of chromophobe-like renal cell carcinoma (RCC) (Figure 1E). Only small bilateral renal cysts were visualised 5 years later, on the 2013 follow up Magnetic Resonance Imaging (MRI). At age 49, in 2015, our patient displayed suspicious para-aortic lymphadenopathies on imaging for which he underwent an aorto-caval lymph node dissection disclosing concurrent RCC metastasis and follicular lymphoma in both nodes identified. As of 2016, at age 51, follow up MRI identified an enlarging left renal complex cystic 1.2 cm lesion with a 0.5 cm enhancing component, suspicious for RCC. The patient is thus currently being followed by the urology service, as well as by haematologists regarding his follicular lymphoma. Additionally, a 2012 chest CT identified fatty lesions most suggestive of TSC-associated myocardial fatty foci (MFF), further characterised by cardiac MRI in 2017 [4–6]. The proband's personal history otherwise also includes three melanocytic nevi resected from his thorax, shoulder, and arm at age 40, a dysplastic junctional melanocytic nevus at age 41, as well as an intrastromal melanocytic nevus of the right bulbar

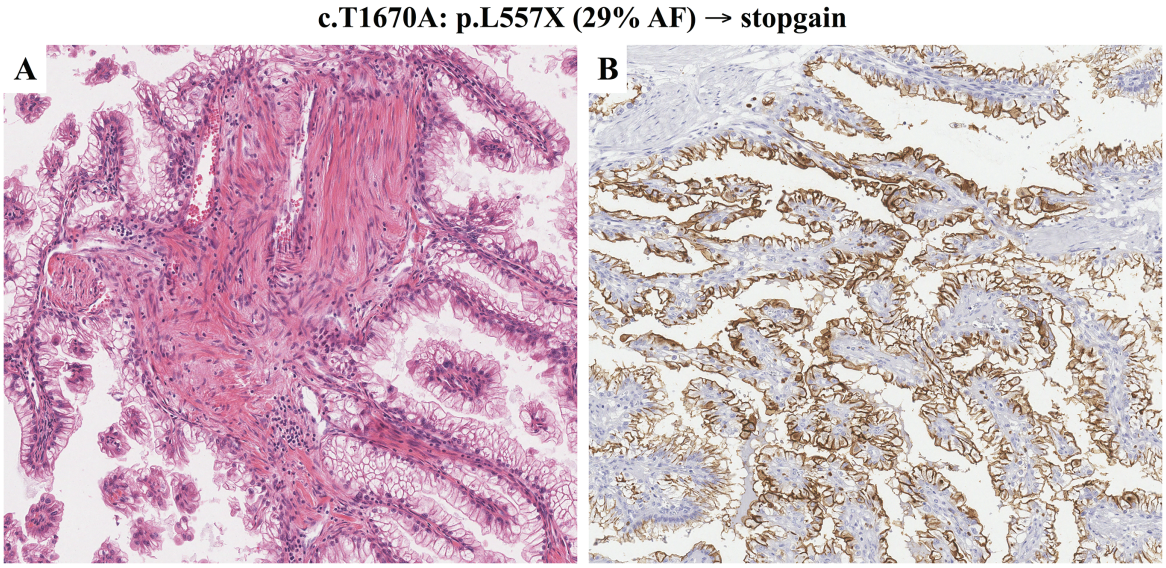

Figure 2. RCCLS resected in the proband's mother at the age of 60. This papillary proliferation of cells with glycogen-rich, clear cytoplasm exhibits focally aggregated stromal smooth muscle fibres [(A) H&E stain]. Note the diffuse cell membrane immunohistochemical positivity for CD10, which helps further in discriminating this neoplasm from clear cell papillary RCC (B).

conjunctiva with microcysts and a right arm lipoma both resected at age 43. On physical examination, numerous brachial and thoracic infracentimetric hypopigmented macules had been noted, accentuated under Wood's lamp (supplementary material, Figure S3). The same cutaneous lesions were allegedly present in the proband's sister and grandmother, in addition to being documented in his son. The index case also displayed prominent facial sebaceous glands on macroscopic clinical assessment.

Review of the family history showed the proband's mother to have presented at age 60 with similar RCCLS tumour on a background of multifocal leiomyomatous angiomyolipomas (AMLs) (Figure 2), followed by melanoma at 65, which metastasized and caused her demise at 67. The proband's sister was diagnosed with RCC at age 43 (identified subsequently to the tumours in the index case), his maternal half-brother was known for epilepsy and died accidentally at age 21, and both the proband's father and sister were known for renal cysts, while his son had two seizure episodes at the age of 4, with an unremarkable brain MRI at that time and at age 11. Following a diagnosis of tuberous sclerosis in his father, he was found to have hypopigmented macules and ash leaf lesions.

Material and methods

To confirm a diagnosis of TSC, we tested the proband for *TSC1/TSC2* gene alterations via massive parallel sequencing of peripheral blood [Illumina (San Diego, CA, USA), GeneDx (Gaithersburg, MD, USA) proprietary targeted capture]. Additionally, using core biopsies of formalin-fixed, paraffin-embedded (FFPE) archival tissues, we performed whole-exome sequencing (WES) of all five resected RCCs from the index case, as well as the RCC resected in his mother, with corresponding FFPE normal tissue controls. Bioinformatic analysis of exome sequencing data was performed using our WES pipeline as previously described [7,8]. In brief, sequenced reads were trimmed and mapped to the reference genome (hg19) using trimmomatic (v.0.35) and Burroughs-Wheeler aligner (v.0.5.9), respectively [9]. After mapping, GATK [10] and Picard (http://broadinstitute.github.io/picard//) were used to perform local realignment around small insertions and deletions (indels) and to mark read duplicates. Then, GATK was applied to assess capture efficiency and coverage for all samples. A mean coverage of 114.4X (ranging from 41.6X to 156.4X) was obtained for all consensus coding sequences (CCDS) and 98.1% and 95.8% of CCDS bases are covered by at least 5 and 20 reads, respectively (supplementary material, Table S1). Samtools (v. 0.1.18) [11] and ANNOVAR [12] were used for variants calling [single nucleotide variants (SNVs) and indels] and functional annotations, respectively [12]. To remove common variants and false positive calls, candidate mutations were subjected to several filtering steps and eliminated if they fulfilled any one of the following criteria: (i) genomic position of variant covered by <5X, (ii) <4

Table 1. Tumour-specific *TSC2* alterations in various RCCs as per WES

RCC tumour	RCC histotype	*TSC2* alteration on WES
Mother's RCC	RCCLS	c.T1670A: p.L557X (29% AF) stopgain
RCC #1	RCCLS	c.G4537T: p.E1513X (32% AF) stopgain
RCC #2	RCCLS	Undetected
RCC #3	RCCLS	Allelic imbalance (75% AF)
RCC #4	RCCLS	c.351_352del:p.G117 fs (27% AF) frameshift deletion
RCC #5	Chromophobe-like	Allelic imbalance (72% AF)

AF, Allelic frequency.

reads support the alternative variant, (iii) variant has allelic ratio <10% for SNVs or <15% for indels, (iv) variant has allele frequency >0.001 in ExAC databases, or seen as homozygote in ExAC database. Finally, only the most likely damaging variants (nonsense, canonical splice-site, missense, and coding indels) were considered; variants in non-coding regions, synonymous variants and variants present in highly repetitive regions were excluded from further analysis. The manual examination of all potential candidate variants, predicted to be deleterious by at least three of six bioinformatics algorithms (SIFT, PolyPhen, MutationTaster, Revel, CADD, and MCAP), was performed using IGV [13]. Somatic SNVs and Indels were identified using MuTect (see https://confluence.broadinstitute.org/display/CGATools/MuTect for method) and Indelocator (for method, see https://confluence.broadinstitute.org/display/CGATools/Indelocator) respectively, and were then annotated with ANNOVAR. Allelic Imbalance (AI) analysis was performed by ExomeAI as previously described [14]. In brief, ExomeAI detects AI events across samples using all heterozygous variants [B-allele frequency (BAF) values of 0.05–0.95] extracted from variant call format files to detect AI events across samples; the circular binary segmentation algorithm was applied to identify the derived segments. Binomial and Wilcoxon signed rank tests were used to evaluate the significant of each segment [14]. This study was approved by the Institutional Review Board of the Faculty of Medicine of McGill University, Montreal, QC, Canada, no. A08-M61-A09B, and informed consent was obtained from each patient.

Results

The index case's germline was shown to harbour a heterozygous *TSC2* c.2714 G > A, (p.Arg905Gln), (R905Q) missense pathogenic variant following massive parallel sequencing of peripheral blood (Illumina, GeneDx proprietary targeted capture), with confirmation via capillary sequencing. This mutation has been acknowledged to be pathogenic in various publications (detailed in the 'Discussion' section below) [15]. The proband's son and sister were shown to be heterozygous for the same pathogenic germline variant, warranting regular clinical follow up with the neurology service, with this same mutation being also demonstrated in the proband's mother by WES of non-neoplastic FFPE tissue. Among the RCCs sampled in both the index case and his mother, all except one displayed either unique tumour-specific deleterious second hits in *TSC2*, or significant AI at the *TSC2* gene locus on chromosome 16 (Table 1 and supplementary material, Figure S4). As expected, all FFPE RCC samples harboured the mutation previously demonstrated in the proband's blood. In addition, we detected no truncating mutations in an array of 114 cancer predisposition genes as collated by Rahman (supplementary material, Table S2) [16]. No significant alterations were detected among the array of less well-known genes previously observed to be mutated by Tyburczy *et al* in the context of TSC-associated RCCs secondary to *TSC2* second hits (*SDHB*, *RASA1*, *TACC3*, *PROS1*, *NPFFR2*, *XYLT1*, *GALNTL6*, *NUP214*, *GLUD2*, *USP34*, *MS4A7*, *NDE1*, *ZNF507*, *ZRANB1*, *PANX1*, *PHF20*, *PNISR*) [17]; nor were any *TCEB1* gene mutations detected [18].

Discussion

While the commonest TSC clinical findings are usually cutaneous and neurological, our index case's phenotype is atypical in that no significant neurological abnormalities were documented throughout various investigations he underwent through the years, and he presented no sign of epilepsy (bearing in mind that no dedicated brain imaging was performed in him). Regarding TSC cutaneous findings as they pertain to our patient, hypomelanotic macules were shown to be the major cutaneous finding at presentation in 28 of 68 TSC patients in a recent series [19] and are reported in over 90% of TSC patients [2]. Accordingly, a minimum of three hypomelanotic macules over 5 mm in diameter is considered a major criterion sufficient to evoke a possible diagnosis of TSC, according to the International Tuberous Sclerosis Complex Consensus Conference [20]. The proband studied here happened to display scores of smaller 1–2 mm hypopigmented macules ('guttate' or 'confetti macules', 'white freckles'), which are seen

in under 5% of TSC infants and constitute a minor diagnostic criterion of the disease, but are thought to be the pigmentary lesion most specific for TSC (supplementary material, Figure S3) [21]. Another typical cutaneous lesion present in our index case is prominent facial sebaceous glands, usually occurring after puberty in TSC patients [22]. Regarding melanocytic neoplasms as they were observed in the proband and his mother, there have been so far only exceptional reports hinting toward an association between these and TSC [23], which could correlate with the relatively significant 10% prevalence of mTOR pathway alterations in melanoma [24]. Similarly, follicular lymphoma has not been reported to be associated with TSC yet, although 10% of follicular lymphomas were reported to display aberrant mTOR pathway activation in one recent study [25,26]. Further probing for mTOR pathway dysregulation and possible *TSC* gene alterations in both melanocytic lesions and follicular lymphoma may be interesting in that regard. Other present findings significantly correlated with TSC include MFF, which have been reported to be highly specific and 33–50% sensitive for TSC in a limited number of studies [4–6], as well as SBL [3]. On the whole, the TSC phenotype in our index case appears somewhat milder than could be expected in TSC patients in general, with only one cutaneous major diagnostic criterion present in the form of multiple hypomelanotic macules, notable absence of neurological diagnostic criteria, and finally the presence of one other major diagnostic criterion in the form of multiple AMLs, the latter adopting a leiomyomatous-only histology. The attenuated phenotype observed in the family studied here echoes previous reports having associated the *TSC2* R905Q mutation with milder TSC phenotypes [15].

The cutaneous findings mentioned above combined with a history of multiple renal tumours led to further investigations that uncovered an uncommon TSC-associated inherited variant in the proband and his family. Indeed, the *TSC2* exon 23 c.2714 G > A, p.Arg905Gln (R905Q) missense mutation is a rare pathogenic variant seen in under 1% of TSC patients (approximately 45 published cases, including 25 within a single family). It has been documented to be a French Canadian founder mutation resulting in reduced tuberin function and characteristically mild TSC phenotypes with little intrafamilial phenotypic variability, as studied in 19 TSC families by Jansen *et al* in 2006 [15]. This specific *TSC2* R905Q pathogenic germline variant occurs at a methylated CpG site through a C to T deamination reaction, and was shown to lead to tuberin instability via increased interaction with HERC1 ubiquitin ligase, which interaction would not be blocked by TSC1 as it is in wild-type patients, resulting in increased TSC2 ubiquitination [27].

In our proband's family, TSC-related kidney neoplasms in the form of AML and RCCLS were observed across two generations. Regarding kidney lesions in general, modified smooth muscle cells of the renal capsule have the potential to engender smooth muscle outgrowths and neoplasms. For instance, lymphangioleiomyomatosis secondary to *TSC2* mutations, arising most frequently in the lung, can also develop in the kidney [28]. In the context of tuberous sclerosis, AML is the most common renal neoplasm encountered, affecting 80% of patients, usually as of the age of 10 [29]. While exhibiting a standard AML immunophenotype, some of these lesions adopt an exclusively leiomyomatous histology [30,31], as seen in the proband and his mother. RCC appears earlier and often multifocally in TSC patients [32], often with concurrent AML [33], but at an incidence of approximately 2%, roughly comparable to that of the general population [34,35]. Interestingly, a *TSC2* variant was first reported to be associated with multiple bilateral RCCs by Tyburczy *et al* in 2015 in two unrelated individuals [17], and it is the exact same variant in *TSC2* (p.R905Q) we have detected in three related RCC-affected individuals including one patient with multiple bilateral tumours. Our findings thus strengthen the association between TSC and multiple bilateral RCCs. Regarding specific RCC histotypes, 30% of TSC-associated RCCs display prominent intrinsic smooth muscle proliferation and clear cell cytology, a histological aspect designated 'renal cell carcinoma with (angio)leiomyomatous stroma' (RCCLS), this RCC subtype being commoner in TSC patients as opposed to the general population [36]. This distinct association of TSC with RCCLS explains that, among RCCLS tumours in general, 35% have been reported to be associated with TSC (6/17 RCCLS tumours), half of which could represent the sentinel manifestation for a TSC diagnosis (3/6 RCCLS in Verkarre's 2014 study) [37]. While RCCLS and clear cell papillary RCC are considered by the International Society for Urological Pathology to potentially represent the ends of one lesional spectrum, only RCCLS is diffusely positive for CD10, as was the case in both the proband and his mother (Figure 2) [31,36]. Of note, this same RCCLS subtype has been documented to display aberrant Succinate Dehydrogenase B (SDHB) negativity on immunohistochemistry, similarly to the succinate dehydrogenase-deficient RCC subtype, although in the absence of detectable deleterious *SDHB* genetic alterations that portend the development of SDHB-

deficient RCCs [38]. Indeed, a recent study linked SDHB IHC signal rarefaction in RCCLS to decreased mitochondrial density as assessed by electron microscopy [39]. As expected, no likely pathogenic or clearly pathogenic *SDHB* alterations were detected among our RCC samples studied via massive parallel sequencing. In non-TSC individuals, some RCCLS tumours have been shown to harbour *TCEB1* mutations [18], this being followed by HIF-1α activation as is also observed in TSC-associated RCCLS [40]. As would be expected in TSC-affected relatives, the five RCCLS tumours that underwent WES displayed no *TCEB1* mutation (either nonsense, canonical splice-site, missense, or coding indels). Most notably, none of the Y79C/S/F/N or A100P hot-spot mutations were detected. Otherwise, among all histotypes encountered in TSC-associated RCC, the most prevalent is a chromophobe-like RCC that shows phenotypic similarities to the eosinophilic variant of chromophobe RCC. This chromophobe-like RCC represents 60% of TSC-associated RCCs [36], and one of our proband's tumours corresponded to that phenotype (Figure 1E).

The *TSC2* R905Q pathogenic germline variant seems to have carried an increased RCC risk in the present index case, his mother as well as his sister, particularly regarding RCCLS, which has developed in the first two relatives, including five occurrences in our proband. Genetically speaking, TSC-associated smooth muscle proliferations like AMLs (28/30 tumours) [32,41] as well as more aggressive smooth muscle-rich proliferations such as RCCLS tumours have been shown to result from second hits in *TSC1/2*, as shown by Tyburczy *et al* on 5/5 fresh frozen RCCs and 6/7 RCCs in total [17]. In the context of the same background *TSC2* R905Q pathogenic germline variant, we have been able to reproduce this finding using WES in 5/6 different FFPE RCCs from the index case and his mother. *TSC1/2* second hits seem even more pivotal as a tumourigenic mechanism in TSC considering that they have been detected in angiofibromas arising in TSC patients [42]. Our demonstration of unique tumour-specific *TSC2* deleterious second hits/AI in multiple bilateral RCCs including a high proportion of RCCLS tumours supports the notion that RCCLS may be strongly related to abnormalities of the mTOR pathway [32]. The molecular driver could well be the same in both TSC-associated RCCs and their non-familial equivalents, and we hypothesize that mTOR pathway alterations are likely to play a significant role in the tumourigenesis of non-familial RCCLS as well. This mechanistic foray into RCCLS pathogenesis further emphasizes the relevance of a molecular classification of different RCCs. Additionally, we believe that the high prevalence of RCCLS tumours in our index case raises the question whether this RCC subtype should be included as a minor criterion for the diagnosis of TSC.

Our study's limitations include our inability to retrieve, sequence, and review the histology of the sole RCC resected in the proband's sister, which may have allowed us to show further similarities between this tumour and other RCCs we analysed. Given the relatively low population prevalence of TSC and of this particular *TSC2* pathogenic germline variant more specifically, the number of patients studied herein is limited, which restricts one's ability to make statistically powerful inferences pertaining to the whole of TSC patients with a similar genotype/phenotype (external validity).

This confirmatory study highlights the key tumourigenic role of tumour-specific *TSC2* second hits in TSC-associated RCCs. The *TSC2* R905Q along with other TSC variants may furthermore specifically lead to increased frequency of the RCC histotype known as RCCLS, as this neoplasm was observed to make up a notably large proportion of the renal malignancies resected in both our index case and his mother (5/6 neoplasms). In all events, one should stress the importance of recognizing this uncommon RCC histotype and of distinguishing it from clear cell papillary RCC, as it is becoming more and more apparent that RCCLS may present as a sentinel anomaly in TSC patients with atypical phenotypes [37]. These data further emphasize the relevance of a molecular classification of both familial and sporadic RCC, as well as the potential benefits of mutation-specific management and counselling for TSC patients.

Acknowledgements

The authors thank the patients for participating in this study. This work was supported by a grant from the Canadian Institutes of Health Research (FDN-148390) to WDF.

Author contributions statement

WDF and IB designed the study. IB, WDF, LRB, SF, MDA, ST, and NH collected data. WDF, IB and NH conceived experiments. IB and NH carried out experiments. IB, WDF, LRB, SF, and NH analysed and interpreted data. IB and LRB performed literature search. IB generated figures. IB and SF drafted the manuscript. All authors were involved in the

manuscript revision and had final approval of the submitted and published versions.

References

1. Sampson JR, Scahill SJ, Stephenson JB, *et al*. Genetic aspects of tuberous sclerosis in the west of Scotland. *J Med Genet* 1989; **26:** 28–31.
2. DiMario FJ Jr, Sahin M, Ebrahimi-Fakhari D. Tuberous sclerosis complex. *Pediatr Clin North Am* 2015; **62:** 633–648.
3. Brakemeier S, Vogt L, Adams LC, *et al*. Sclerotic bone lesions as a potential imaging biomarker for the diagnosis of tuberous sclerosis complex. *Sci Rep* 2018; **8:** 953.
4. Tresoldi S, Munari A, Di Leo G, *et al*. Myocardial fatty foci in adult patients with tuberous sclerosis complex: association with gene mutation and multiorgan involvement. *Radiology* 2015; **277:** 398–405.
5. Adriaensen ME, Schaefer-Prokop CM, Duyndam DAC, *et al*. Fatty foci in the myocardium in patients with tuberous sclerosis complex: common finding at CT. *Radiology* 2009; **253:** 359–363.
6. Shaaya EA, Hirshberg JS, Rabe OT, *et al*. Cardiac fat-containing lesions are common in tuberous sclerosis complex. *Am J Med Genet A* 2013; **161A:** 1662–1665.
7. Fahiminiya S, Majewski J, Mort J, *et al*. Mutations in WNT1 are a cause of osteogenesis imperfecta. *J Med Genet* 2013; **50:** 345–348.
8. Fahiminiya S, Al-Jallad H, Majewski J, *et al*. A polyadenylation site variant causes transcript-specific BMP1 deficiency and frequent fractures in children. *Hum Mol Genet* 2015; **24:** 516–524.
9. Li H, Durbin R. Fast and accurate short read alignment with Burrows-Wheeler transform. *Bioinformatics* 2009; **25:** 1754–1760.
10. McKenna A, Hanna M, Banks E, *et al*. The Genome Analysis Toolkit: a MapReduce framework for analyzing next-generation DNA sequencing data. *Genome Res* 2010; **20:** 1297–1303.
11. Li H, Handsaker B, Wysoker A, *et al*. The Sequence Alignment/Map format and SAMtools. *Bioinformatics* 2009; **25:** 2078–2079.
12. Wang K, Li M, Hakonarson H. ANNOVAR: functional annotation of genetic variants from high-throughput sequencing data. *Nucleic Acids Res* 2010; **38:** e164.
13. Robinson JT, Thorvaldsdóttir H, Winckler W, *et al*. Integrative genomics viewer. *Nat Biotechnol* 2011; **29:** 24–26.
14. Nadaf J, Majewski J, Fahiminiya S. ExomeAI: detection of recurrent allelic imbalance in tumors using whole-exome sequencing data. *Bioinformatics* 2015; **31:** 429–431.
15. Jansen AC, Sancak O, D'Agostino MD, *et al*. Unusually mild tuberous sclerosis phenotype is associated with TSC2 R905Q mutation. *Ann Neurol* 2006; **60:** 528–539.
16. Rahman N. Realizing the promise of cancer predisposition genes. *Nature* 2014; **505:** 302–308.
17. Tyburczy ME, Jozwiak S, Malinowska IA, *et al*. A shower of second hit events as the cause of multifocal renal cell carcinoma in tuberous sclerosis complex. *Hum Mol Genet* 2015; **24:** 1836–1842.
18. Hakimi AA, Tickoo SK, Jacobsen A, *et al*. TCEB1-mutated renal cell carcinoma: a distinct genomic and morphological subtype. *Mod Pathol* 2015; **28:** 845–853.
19. Nathan N, Burke K, Moss J, *et al*. A diagnostic and management algorithm for individuals with an isolated skin finding suggestive of tuberous sclerosis complex. *Br J Dermatol* 2017; **176:** 220–223.
20. Northrup H, Krueger DA, Northrup H, *et al*. Tuberous sclerosis complex diagnostic criteria update: recommendations of the 2012 International Tuberous Sclerosis Complex Consensus Conference. *Pediatr Neurol* 2013; **49:** 243–254.
21. Jóźwiak S, Schwartz RA, Janniger CK, *et al*. Skin lesions in children with tuberous sclerosis complex: their prevalence, natural course, and diagnostic significance. *Int J Dermatol* 1998; **37:** 911–917.
22. Tsao H, Luo S. Neurofibromatosis and tuberous sclerosis. In *Dermatology* (3rd edn), Bolognia J, Jorizzo JL, Schaffer JV (Eds). Elsevier: Philadelphia, PA, 2012; 925–941.
23. Ceylan C, Ozdemir F, Ozturk G, *et al*. Tuberous sclerosis associated with multiple speckled lentiginous nevi. *J Eur Acad Dermatol Venereol* 2003; **17:** 616–617.
24. Kong Y, Si L, Li Y, *et al*. Analysis of mTOR gene aberrations in melanoma patients and evaluation of their sensitivity to PI3K-AKT-mTOR pathway inhibitors. *Clin Cancer Res* 2016; **22:** 1018–1027.
25. Ying ZX, Jin M, Peterson LF, *et al*. Recurrent mutations in the MTOR regulator RRAGC in follicular lymphoma. *Clin Cancer Res* 2016; **22:** 5383–5393.
26. Leseux L, Laurent G, Laurent C, *et al*. PKC zeta mTOR pathway: a new target for rituximab therapy in follicular lymphoma. *Blood* 2008; **111:** 285–291.
27. Chong-Kopera H, Inoki K, Li Y, *et al*. TSC1 stabilizes TSC2 by inhibiting the interaction between TSC2 and the HERC1 ubiquitin ligase. *J Biol Chem* 2006; **281:** 8313–8316.
28. Merino MJ. What is new in renal pathology? *Int J Surg Pathol* 2010; **18:** 98s–100s.
29. Islam MP, Roach S. Neurocutaneous syndromes. In *Bradley's Neurology in Clinical Practice* (7th edn), Daroff RB, Jankovic J, Mazziotta JC, Pomeroy SL, Bradley WG (Eds). Elsevier: Philadelphia, PA, 2016; 1538–1562.
30. Nikaido T, Nakano M, Kato M, *et al*. Characterization of smooth muscle components in renal angiomyolipomas: histological and immunohistochemical comparison with renal capsular leiomyomas. *Pathol Int* 2004; **54:** 1–9.
31. Srigley JR, Delahunt B, Eble JN, *et al*. The International Society of Urological Pathology (ISUP) Vancouver classification of renal neoplasia. *Am J Surg Pathol* 2013; **37:** 1469–1489.
32. Lam HC, Nijmeh J, Henske EP. New developments in the genetics and pathogenesis of tumours in tuberous sclerosis complex. *J Pathol* 2017; **241:** 219–225.
33. Rakowski SK, Winterkorn EB, Paul E, *et al*. Renal manifestations of tuberous sclerosis complex: incidence, prognosis, and predictive factors. *Kidney Int* 2006; **70:** 1777–1782.
34. Dixon BP, Hulbert JC, Bissler JJ. Tuberous sclerosis complex renal disease. *Nephron Exp Nephrol* 2011; **118:** e15–e20.
35. Ljungberg B, Campbell SC, Cho HY, *et al*. The epidemiology of renal cell carcinoma. *Eur Urol* 2011; **60:** 615–621.
36. Guo J, Tretiakova MS, Troxell ML, *et al*. Tuberous sclerosis-associated renal cell carcinoma: a clinicopathologic study of 57 separate carcinomas in 18 patients. *Am J Surg Pathol* 2014; **38:** 1457–1467.
37. Verkarre V, Leroy X, Sibony M, *et al*. Étude anatomo-clinique rétrospective d'une série de 17 cas de carcinomes rénaux à stroma leiomyomateux identifiant une association forte avec la Sclérose Tubéreuse de Bourneville. *Prog Urol* 2014; **24:** 835–836.

38. Yang P, Cornejo KM, Sadow PM, *et al*. Renal cell carcinoma in tuberous sclerosis complex. *Am J Surg Pathol* 2014; **38:** 895–909.
39. Williamson SR, Hornick JL, Eble JN, *et al*. Renal cell carcinoma with angioleiomyoma-like stroma and clear cell papillary renal cell carcinoma: exploring SDHB protein immunohistochemistry and the relationship to tuberous sclerosis complex. *Hum Pathol* 2018; **75:** 10–15.
40. Liu MY, Poellinger L, Walker CL. Up-regulation of hypoxia-inducible factor 2alpha in renal cell carcinoma associated with loss of Tsc-2 tumor suppressor gene. *Cancer Res* 2003; **63:** 2675–2680.
41. Giannikou K, Malinowska IA, Pugh TJ, *et al*. Whole exome sequencing identifies TSC1/TSC2 biallelic loss as the primary and sufficient driver event for renal angiomyolipoma development. *PLoS Genet* 2016; **12:** e1006242.
42. Tyburczy ME, Wang J-A, Li S, *et al*. Sun exposure causes somatic second-hit mutations and angiofibroma development in tuberous sclerosis complex. *Hum Mol Genet* 2014; **23:** 2023–2029.

SUPPLEMENTARY MATERIAL ONLINE

Figure S1. Multiple osseous hyperdense, sclerotic lesions (blue circles) are visualized on computed tomography imaging, having remained stable since first imaged 9 years ago, in keeping with TSC-associated sclerotic bone lesions (2015 chest, abdomen, and pelvis CT scan with contrast)

Figure S2. Upper lobes of the lungs display multiple ground glass nodular densities (blue circles) on computed tomography imaging, which have remained stable since first imaged 9 years ago, most likely corresponding to multifocal micronodular pneumocyte hyperplasia (MMPH) (2014 chest CT scan with contrast)

Figure S3. Numerous infracentimetric hypopigmented macules can be noted on the proband's back. These lesions were accentuated under Wood's lamp. The same cutaneous lesions were allegedly present in the proband's sister and grandmother, in addition to being documented in his son

Figure S4. The BAF profiles on chromosome 16 are shown for two RCC samples with AI. Each point on the plot represents a heterozygote variant and the position-wise significant loci are in orange. The *x*-axis shows the genomic positions in Mb. The *y*-axis indicates either BAF (for all points as well as the red bars) or absolute deviation of BAF from 0.5 (only for the segments in blue). For each significant segment, there are two red bars showing the mean of the BAF (for BAF > 0.5 and BAF < 0.5) for that segment

Table S1. Sequencing coverage

Table S2. Variant filtering strategy and identification of *TSC2* mutations